Thermodynamics of second phase conductive filaments

V. G. Karpov, M. Nardone,[a] and M. Simon
Department of Physics and Astronomy, University of Toledo, Toledo, Ohio 43606, USA

(Received 28 March 2011; accepted 3 April 2011; published online 6 June 2011)

We present a theory of second phase conductive filaments in phase transformable systems; applications include threshold switches, phase change memory, resistive memory, and shunting in thin film structures. We show that the average filament parameters can be described thermodynamically. In agreement with the published data, the predicted filament current-voltage characteristics exhibit negative differential resistance that vanishes at high currents where the current density becomes a bulk material property. Our description is extendible to filament transients and allows for efficient numerical simulation. © *2011 American Institute of Physics*. [doi:10.1063/1.3592983]

I. INTRODUCTION

A general observation common to multiple modern technologies is that thin-film structures can drastically decrease their transverse electrical resistance by forming second phase conductive filaments (SPCFs) in response to electric bias. These SPCFs represent cylinder shaped inclusions that are structurally and/or chemically different from the host material, such as, e.g., crystalline SPCFs that punch through insulating amorphous hosts in chalcogenide phase change memory, metallic filaments in insulating films of resistive memory, or defect constituted SPCFs through thin film insulating oxides. SPCFs can be either stable, as in phase change memory and dielectric oxides after hard breakdown, or unstable (disappearing after the bias is removed or proper annealing), as in threshold switches[1] and some thin film structures. From a practical perspective, SPCFs can cause detrimental shunting and loss of functionality in devices such as thin-film photovoltaics and thin oxides of electronic devices.[2,3] On the other hand, in implementations such as threshold switches,[4,5] phase change memory,[6] and resistive memory,[7] SPCFs facilitate information storage and logic operations.

Despite a long history of observations, a theoretical framework for SPCFs does not exist. Here, we introduce a general thermodynamic theory that describes SPCFs coupled with an external circuit (sometimes referred to as global coupling) and predicts the SPCF radius as a function of the electric current and material parameters, as well as the corresponding current-voltage (IV) characteristics. Our theory is conceptually applicable at any size scale (to within the thermodynamic approximation) and over the full IV range. A finite element numerical simulation is employed to support our analytical results, which are found to be in excellent agreement with the data.

For specificity we consider the archetypal SPCF system of chalcogenide glass threshold switches wherein reversible switching takes place between highly resistive (amorphous) and conductive (SPCF) phases. They have recently regained interest in connection with 3D stackable phase change memory.[5] The empirical fact that the SPCF radius increases with current as $r \propto I^{1/2}$ has been known[4,8] since the seminal work by Ovshinsky,[1] yet it still lacks a theoretical description. An early approach based on the principle of least entropy production[9] did not result in verifiable predictions; its validity remains questionable[10] and avoidance of it leads to different results, as shown here.

To avoid any misunderstanding, it may be worth noting that our theory here is not related to the well developed theory of current filamentation in bistable semiconductors (see, e.g., Refs. 11–14, and references therein). Several important differences can be pointed out. The latter theories proceed from the premise of a spatiotemporal differential equation for a distributed characteristic (charge carrier concentration, temperature, etc.) complimented with the current voltage characteristic of the entire system that is taken to be multivalued (S-shaped, etc.). They do not include any concepts of phase transformations, such as the change in chemical potential and interfacial energy. These theories then show the conditions under which, near equilibrium, the filament remains stable, or decaying, or oscillating, or even traveling in lateral directions. The corresponding results are typically limited to within close proximity of equilibrium.

On the contrary, our theory presented here does not imply any global current voltage characteristics nor does it postulate any spatiotemporal differential equations. Instead, we proceed from the classical phase transition concepts, explicitly including the difference in chemical potentials and interfacial energy between the two phases. Based on the known approaches to nucleation kinetics, our theory then provides an approximate equation describing the filament evolution in terms of free energy that includes the contributions from phase transformations, Joule heat, and electrostatics. This approach generates results applicable in the full range of filament and host material parameters, including far from equilibrium, predicting the current-voltage characteristic of the filament as well as the relation between its radius and the current. While approximate (neglecting fluctuations between filaments), our results are verified by substituting specific material parameters and comparing to the published experimental data; the agreement is excellent without adjusting parameters.

This paper is organized as follows. Section II describes our general approach where the Fokker–Planck equation is

[a]Electronic mail: Marco.Nardone@utoledo.edu.

used to derive the equation for evolution of the filament average parameters. In Sec. III a simple system with flat electrodes is introduced as a model that adequately describes the free energy. The analysis of steady state filaments is presented in Sec. IV. In Sec. V we discuss the numerical values of filament parameters for a specific case of SPCFs in chalcogenide switches. There, we also describe our developed numerical analysis of switching phenomenon implemented with COMSOL software. Section VI briefly introduces the results of a linear stability analysis that provides the conditions under which the filament will grow, decay, or oscillate. Our conclusions are summarized in Sec. VII.

II. GENERAL FORMALISM

Whether electronic[15,16] or crystalline,[17] or otherwise different from the host material, an SPCF represents a domain of different phase, thus calling upon the analysis of phase transformations. Our conservative approach avoids the principle of least entropy production starting instead with the kinetic Fokker–Planck equation, the applicability of which to phase transformations, particularly to nucleation phenomena (according to Zeldovich theory), is well established.[18] Following that approach (see, e.g., p. 428 in Ref. 18) the Fokker–Planck equation in the space of cylinder radii r takes the form

$$\frac{\partial f}{\partial t} = -\frac{\partial s}{\partial r}, \quad s \equiv -B\frac{\partial f}{\partial r} + Af = -Bf_0\frac{\partial}{\partial r}\left(\frac{f}{f_0}\right). \tag{1}$$

Here, f is the distribution function so that $f(r)dr$ gives the concentration of filaments in the interval $(r, r+dr)$; s is the flux in radii space (s^{-1} cm^{-3}). The "filament radius diffusion coefficient" B can be estimated as $\nu a^2 \exp(-W_a/kT)$ where ν is the characteristic atomic frequency ($\sim 10^{13}$ s^{-1}), a is the characteristic interatomic distance, W_a is the kinetic phase transformation barrier, k is Boltzmann's constant, and T is the temperature. A is connected with B by a relationship which follows from the fact that $s=0$ for the equilibrium distribution $f_0(r) \propto \exp[-F(r)/kT]$, where F is the free energy.

We note that the concept of free energy F that appears with the equilibrium distribution f_0 is not compromised by the fact that electric current flows through the SPCFs, since that current is fixed by the external circuit and serves only as a temperature source. Hence, F describes the free energy of the SPCFs in an insulating host parametrically dependent on the electric current. In other words, ours is not a case of equilibrium thermodynamics used to describe a dissipative system. Many similar examples can be conceived where a system remains nondissipative in spite of the temperature being maintained by an extraneous source of current Joule heat.

Two boundary conditions to Eq. (1) are imposed as follows. The boundary condition $f(r=0)=0$ reflects the fact that very thin filaments cannot exist due to limitations such as loss of conductivity or mechanical instability (extraneous to the present model). Another condition, $f(r=\infty)=0$, implies that only finite radii are achievable over finite times t.

Using the right-hand-side expression for s, multiplying Eq. (1) by r, integrating from 0 to ∞ by parts, and noting that $\int f r dr = \langle r \rangle$, yields $\partial\langle r\rangle/\partial t = \langle \partial F/\partial r\rangle$ (angle brackets denote averages). We then approximate $\langle F\rangle = F(\langle r\rangle)$ and $\langle \partial F/\partial r\rangle = \partial\langle F\rangle/\partial\langle r\rangle$, thereby neglecting fluctuations in the ensemble of nominally identical filaments. Omitting for brevity the angle brackets, one finally obtains

$$\frac{\partial r}{\partial t} = -b\frac{\partial F}{\partial r} \quad \text{with} \quad b = \frac{B}{kT}. \tag{2}$$

This equation which expresses the average evolution of SPCFs cylinder radius has the standard meaning of a relation between the (growth) velocity and the (thermodynamic) force $-\partial F/\partial r$, with the mobility b and the diffusion coefficient B obeying the Einstein relation.

In what follows we consider mostly the steady state case $\partial r/\partial t = 0$, which, according to Eq. (2), takes place when the F is a minimum (obviously different from the condition of least entropy production).[9] However, in principle, Eq. (2) is capable of describing various transients; this will be illustrated in Sec. VI.

III. FLAT ELECTRODE MODEL

To analytically present the free energy we consider a model in Fig. 1 based on a flat plate capacitor of area A and thickness h containing a cylindrical SPCF of radius r. In what follows we will assume the characteristic filament dimensions well above the screening length, thereby neglecting possible effects due to electric charge redistribution around the SPCFs. Including these effects would result in additional terms to the free energy, adding mathematical complexity while not changing the approach of this work.

With the above in mind, the major part of the free energy is given by

$$F = c\delta T \pi r^2 h + \frac{CU^2}{2} + 2\pi r h\sigma + \pi r^2 h\mu. \tag{3}$$

Here, c is the specific heat of the SPCFs, δT is the current dependent temperature change, U is the voltage across the capacitor, $C = \varepsilon A/4\pi h$, ε is the dielectric permittivity, σ is the surface energy, and μ is the change in chemical potential between the two phases. The first term in Eq. (3) represents the thermal contribution, the second is the electrostatic energy, and the last two correspond to the phase transformation.

For the remainder of this analysis we specify the free energy to the case of SPCFs radii $r > h$ because: (1) published experimental results are available; (2) SPCFs

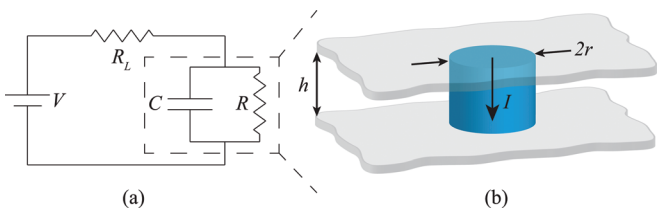

FIG. 1. (Color online) Analytical model components with (a) circuit schematic showing source voltage V, load resistance R_L, capacitance C, and filament resistance R and (b) flat-plate capacitor of height h, and filament of radius r carrying the current I.

dimensions correspond to the above assumed largeness compared to the screening length; and (3) the typical values of the parameters enable one to neglect the second and the third terms in Eq. (5), which allows analytical solutions. In the case of $r > h$, the parameters in Eq. (3) are

$$U = \frac{VR}{R+R_L}, \quad R = \frac{\rho h}{\pi r^2}, \quad \delta T = \frac{I^2 h^2 \rho}{8\pi^2 \kappa c r^4}, \tag{4}$$

where V is the source voltage, R_L is the load resistance, I is the current, R and ρ are the filament resistance and resistivity, respectively, and κ is the thermal diffusivity, taken to be the same for the filament and host materials. The expression for δT follows that of the analysis in Ref. 8.

Substituting Eqs. (4), the free energy becomes

$$F = \frac{3Wh}{2r_0}\left\{\frac{\beta x^2}{(1+Hx^2)^2} + \frac{\gamma}{(1+Hx^2)^2} + x + x^2\right\}, \tag{5}$$

where $x \equiv r/r_0$ and we have introduced the dimensionless parameters

$$\beta = \frac{\pi r_0^3 V^2}{12W\kappa\rho}, \quad \gamma = \frac{r_0}{h}\frac{CV^2}{3W}, \quad H = \frac{R_L \pi r_0^2}{\rho h}. \tag{6}$$

Here the characteristic energy and length

$$W = 16\pi\sigma^3/3\mu^2 \quad \text{and} \quad r_0 = 2\sigma/\mu. \tag{7}$$

would have the physical meaning of nucleation barrier and radius in classical nucleation theory (in which μ is negative and $|\mu|$ is used instead). Assuming σ and $|\mu|$ to be of the same order of magnitude as for crystal nucleation in chalcogenide glasses, one can use the corresponding estimates[19] $W \sim 2$ eV and $r_0 \sim 3$ nm.

IV. STEADY STATE FILAMENT

The free energy of Eq. (5) as a function of filament radius for various source voltages is illustrated in Fig. 2(a). The curves indicate that the filament can exist in a long-lived metastable state at $x = x_f$ [i.e., with the right minimum shallower than the left one at $F(x=0)$]. It becomes stable (i.e., the right minimum energy negative) at relatively high voltages, $V > (h^2/CR_L)\sqrt{3W\rho/\pi r_0^3\kappa}$. On the other hand, finite

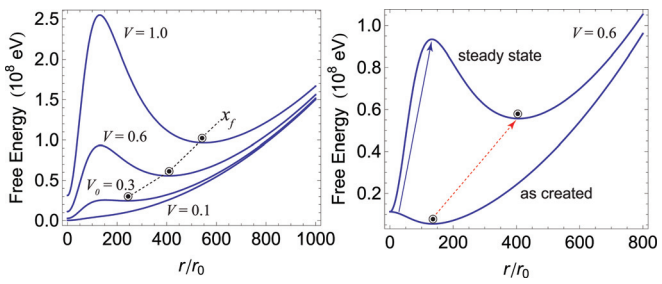

FIG. 2. (Color online) (a) Typical free energy vs filament radius $x = r/r_0$ at various source voltages V [from Eq. (5)]. The steady state radius is x_f and SPCFs are unstable at $V < V_0$. (b) Free energy of a filament as created (thermal contribution neglected) and in the steady state. Arrows show how the energy minimum moves to the right and becomes metastable, separated by a barrier from the state without the filament.

radius filaments become unstable (i.e., the right minimum disappears) at source voltages below

$$V_0 = 18\sqrt{W\kappa\rho/\pi r_0^3}. \tag{8}$$

V_0 is defined by the conditions $\partial F/\partial r = \partial^2 F/\partial r^2 = 0$ and is presented by the curve labeled 0.3 V in Fig. 2(a).

At $V = V_0$, the steady state SPCF radius takes on its minimum value,

$$r_{\min} = r_0\sqrt{2/H} = \sqrt{2\rho h/\pi R_L}.$$

The related filament resistance is a maximum, $R_{\max} = \rho h/\pi r_{\min}^2 = R_L/2$. The characteristic holding current, I_h, (below which the SPCF disappears) can be defined as the current attained at the minimum source voltage $V = V_0$ [see the circuit in Fig. 1(a)],

$$I_h = V_0/(R_{\max} + R_L) = 2V_0/3R_L. \tag{9}$$

Along the same lines, the holding voltage is given by $V_h = I_h R_{\max}$, which leads to, $V_h = V_0/3$ (V_h is the voltage across the bulk of the filament and should not be confused with the applied source voltage V_0).

The metastable filament is predicted to be extremely long-lived at source voltages just slightly above V_0. Indeed, as seen from Fig. 2(a), the activation barrier separating the metastable minimum can be as high as $W_B \sim 10^8$ eV. More quantitatively, close to V_0 the shape of the free energy is described by the expansion

$$\delta F = \frac{1}{2!}\frac{\partial^2 F}{\partial x \partial V}|_{V_0, x_{\min}} \delta x \delta V + \frac{1}{3!}\frac{\partial^3 F}{\partial x^3}|_{V_0, x_{\min}} (\delta x)^3,$$

where $x_{\min} = r_{\min}/r_0$, $\delta x = x - x_{\min}$, and $\delta V = V - V_0$ yielding

$$r = r_{\min}\left(1 + \sqrt{\frac{\delta V}{4V_0}}\right), \quad W_B = \frac{4hW}{r_0 H}\left(\frac{\delta V}{V_0}\right)^{3/2}. \tag{10}$$

The large barrier values are due to a large number of particles constituting the filament: $h/Hr_0 \sim hr_{\min}^2/r_0^3 \gg 1$.

As illustrated in Fig. 2(b), the metastable nature of a steady state SPCF does not appear with the filament immediately upon creation [i.e., when the thermal contribution has not yet taken effect and the first term is excluded from Eqs. (3) and (5)]. At

$$V > V_c = \frac{h}{r_0}\sqrt{\frac{3W\rho}{2\pi C R_L r_0}}, \tag{11}$$

the stability of the newly created filament is maintained solely by the field. While that interpretation implies a threshold voltage, it is quantitatively limited by the fact that the present model considers filament creation and disappearance in one step processes, neglecting the possibility of filament nucleation.[21]

Beyond the critical region of voltage close to V_0, the filament radius becomes proportional to $\sqrt{I}$,

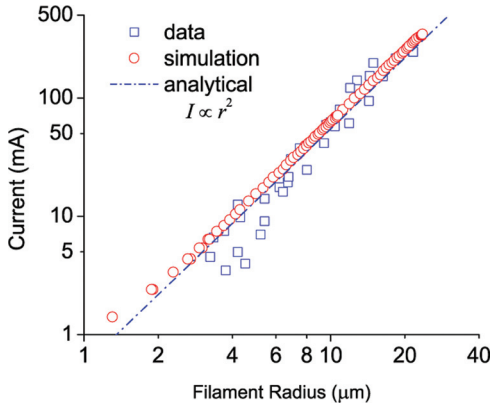

FIG. 3. (Color online) Current as a function of SPCF radius indicating the typical $I \propto r^2$ dependence. Excellent agreement is obtained between the analytical result of Eq. (12), our simulation, and data from Ref. 8.

$$r = r_0\left(\frac{\rho h^2}{12\pi\kappa W r_0}\right)^{1/4}\sqrt{I} \quad \text{when} \quad I \gg I_h, \tag{12}$$

consistent with the above mentioned experimental observations[1,8] (see Fig. 3).

Equation (12) predicts the often observed nearly vertical current voltage characteristic where the device voltage, $V_d = IR \propto I/r^2$, remains constant. The value of this constant voltage at high current, $I \gg I_h$, is given by

$$V_{h\infty} = V_0/3^{3/2} = V_h/\sqrt{3}.$$

The inequality $V_{h\infty} < V_h$ implies a "knee" in IV characteristic and a regime of negative differential resistance (NDR), as shown in Fig. 4(a).

The reason for the apparently infinite differential conductivity $dI/dV \to \infty$ at $V \to V_{h\infty}$ is that, according to Eq. (12), the SPCF automatically adjusts its radius to maintain a constant current density

$$J = \frac{I}{\pi r^2} = \sqrt{\frac{12\kappa W}{\pi\rho r_0^3 h^2}}. \tag{13}$$

The latter current density is a bulk material property and is independent of current. This fact has been known empirically for more than four decades.[1] When the SPCF grows to the device size, saturation is achieved and the current density increases linearly with current [see Fig. 4(b)].

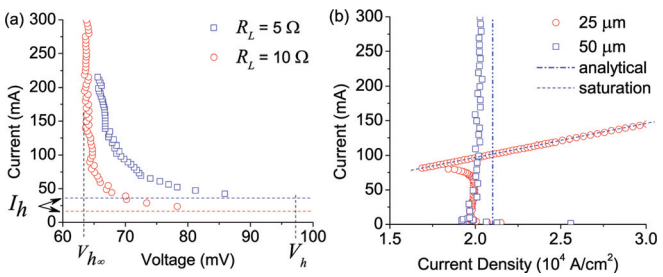

FIG. 4. (Color online) (a) Simulated IV of a filament for the device described in Ref. 8 at two different load resistances R_L. The holding current I_h and voltages $V_{h\infty}$ and V_h are shown. (b) Filament current density for pores (active device regions) of diameters 25 μm and 50 μm. Saturation occurs when the SPCF fills the pore. The results are in good agreement with the data[8] (not shown here).

V. NUMERICAL MODELING

For the typical parameter values $\rho \sim 0.1$ Ω cm, $\kappa \sim 10^{-3}$ cm^2 s^{-1}, $h \sim 3000$ nm, $R_L \sim 100$ Ω, $\varepsilon \sim 10$, and $A \sim 10^{10}$ nm^2,[1,4,8,20] the numerical estimates for the above derived SPCF holding current $I_h \sim 1$ mA and current density $J \sim 10^4$ A/cm^2 are in excellent agreement with the data,[8] without adjusting parameters. On the other hand, the predicted holding voltage $V_h \sim 0.3$ V is considerably lower than the measured $V_h \sim 1$ V.

The latter discrepancy is expected since our model here does not consider blocking electrodes[8,16] that are known to add a current-independent contribution to the voltage across device.[1,4] The physics of such electrodes remains poorly understood; the consensus is that they operate in a fashion of Zener-type diode, possibly due to tunneling through the Schottky type interfacial barrier.[22] The corresponding theory is not very closely related to the subject of this work and will be presented elsewhere. Here, we limit our analysis to including such electrode action on empirical grounds.

To complement our analytical work, finite element numerical simulations were performed using the COMSOL multiphysics package. The electric field and temperature distributions were determined by simultaneously solving the nonlinear, coupled current continuity and heat equations. The results were then integrated to calculate the free energy of Eq. (3). A search algorithm was used to determine the minimum free energy in the parameter space of applied voltage and SPCF radius. The simulations relied on neither the flat-plate capacitor geometry nor the field and temperature approximations of Eq. (4).

Numerous simulations were performed for a broad range of device sizes and geometries. Figures 3 and 4 provide samples of simulation results for the device structure described in Fig. 1 of Ref. 8; overall, very good agreement was obtained without adjusting parameters. The simulation results in Fig. 4(a) clearly indicate the NDR knee in the bottom part of the IV curve, where the SPCF radius increases with I much faster than $\sqrt{I}$. That region of NDR corresponds to the critical region described in our analytical treatment [cf. Eq. (10)].

VI. TIME DEPENDENT FILAMENT

To describe the filament evolution, Eq. (2) should be solved together with the circuit equation corresponding to Fig. 1,

$$C\frac{dU}{dt} = \frac{V}{R_L} - U\left(\frac{1}{R_L} + \frac{1}{R}\right) \tag{14}$$

where U is the voltage across device and R is the device resistance. In general, this does not allow for any simple analytical results.

However, the standard linear stability analysis is straightforward and leads to the equations

$$\frac{d\delta U}{dt} = a_{11}\delta U + a_{12}\delta r, \quad \frac{d\delta r}{dt} = a_{21}\delta U + a_{22}\delta r, \tag{15}$$

where δU and δr are small deviations of U and r from their equilibrium values. The coefficients are given by the expressions

$$a_{11} = -\frac{1}{CR} - \frac{1}{CR_L}, \quad a_{12} = \frac{2U}{RCr},$$
$$a_{21} = -b\frac{\partial^2 F}{\partial r \partial U}, \quad a_{22} = -b\frac{\partial^2 F}{\partial r^2}, \tag{16}$$

with all quantities taken at the steady state condition $\partial F/\partial r = 0$ [see Eq. (2)]. With Eq. (4) and $U = IR$ taken into account, the free energy can be conveniently represented as

$$F = \frac{U^2 hr^2}{8\rho\kappa} + \frac{CU^2}{2} + 2\pi rh\sigma + \pi r^2 h\mu. \tag{17}$$

Reducing Eqs. (15) to a single equation of second order for $\delta U \propto \exp(\lambda t)$, one gets the expression for λ,

$$\lambda = \frac{a_{11} + a_{22}}{2} \pm \sqrt{\frac{(a_{11} + a_{22})^2}{4} + a_{12}a_{21} - a_{22}a_{11}}, \tag{18}$$

which can be either real and positive (decay of the filament with concomitant increase of potential across it) or real and negative (filament growth resulting in the decrease of U), or imaginary (oscillations) depending on the material and circuit parameters included in the coefficients a_{ij}. While all these temporal regimes have been experimentally observed for SPCFs in chalcogenide devices (see Ref. 23, and references therein), and they are generally known for other types of filaments,[13] we note that the range of applicability of the above linear analysis is rather limited. The limitation is due to the fact that the thermally activated mobility coefficient b is exponentially dependent on temperature and thus on the filament radius r and voltage U. This dependence was neglected in the above analysis, since its related contributions to δr and δU appeared in multiplication with $\partial F/\partial r = 0$. However, because of the very strong exponential dependence of $b(r, U)$, the higher powers of δr and δU can become important even when these quantities remain relatively small. The analysis of this situation and the temporal behavior of SPCFs will be presented in more detail elsewhere.

VII. CONCLUSIONS

In conclusion, we have proposed a theory of second phase conductive filaments starting from the basic kinetic approach (Fokker–Planck equation). Our consideration here was based on numerical parameters chosen to make the results verifiable against the comprehensive set of data available for filaments in chalcogenide threshold switches; however the approach remains rather general and extendable to other systems. Our theory is built on the concepts of the classical theory of phase transitions (nucleation), explicitly accounting for the difference in chemical potentials and interfacial energy between two phases; it should not be mixed with the existing theories of current filamentation in semiconductors. More specifically:

(1) For the steady state case, analytical expressions for the average filament radius and current-voltage characteristics have been derived.
(2) Numerical modeling has been developed for the average SPCF characteristics in structures of arbitrary configurations.
(3) Our results correctly predict the filament properties observed in chalcogenide threshold switches, particularly the filament radius versus current, $r \propto \sqrt{I}$, and the corresponding features of their IV characteristics, such as negative differential resistance that vanishes at high currents. The agreement with experimental data is remarkable, without adjusting any parameters.
(4) We have also shown that our approach predicts the observed regimes of filament temporal behavior including growth, decay, and oscillations.

Future work will extend this theory to include more adequate transient analysis beyond the linear stability limitations and specific applications (memory devices, shunting in thin-film photovoltaics, dielectric breakdown, etc.). With respect to threshold switches and phase change memory, it will also be important to explicitly include the effects of Zener-type blocking electrodes that will add a constant voltage component to the predicted current-voltage characteristics.

ACKNOWLEDGMENTS

Useful discussions with Gianpaolo Spadini and Il'ya Karpov are greatly appreciated. We acknowledge the Intel grant supporting our research.

[1] S. R. Ovshinsky, Phys. Rev. Lett. **21**, 1450 (1968).
[2] V. G. Karpov, D. Shvydka, and Y. Roussillon, Phys. Rev. B **70**, 155332 (2004).
[3] M. A. Alam, R. K. Smith, B. E. Weir, and P. J. Silverman, Nature (London) **420**, 378 (2002).
[4] D. Adler, H. K. Henisch, and S. N. Mott, Rev. Mod. Phys. **50**, 209 (1978).
[5] D. C. Kau, S. Tang, I. V. Karpov, R. Dodge, B. Klehn, J. Kalb, J. Strand, A. Diaz, N. Leung, J. Wu, S. Lee, T. Langtry, K. Chang, C. Papagianni, J. Lee, J. Hirst, S. Erra, E. Flores, N. Righos, H. Castro, and G. Spadini, *Proceedings of the IEEE IEDM*, Baltimore (IEEE, New York, 2009), p. 617.
[6] F. Bedeschi, R. Fackenthal, C. Resta, E. M. Donze, M. Jagasivamani, E. C. Buda, F. Pellizzer, D. W. Chow, A. Cabrini, G. Calvi, R. Faravelli, A. Fantini, G. Torelli, D. Mills, R. Gastaldi, and G. Casagrande, IEEE J. Solid-State Circuits **44**, 217 (2009); P. Jovari, I. Kaban, S. Kohara, and M. Takata, Phys. Rev. Lett. **104**, 029901 (2010); M. Krbal, A. V. Kolobov, J. Haines, P. Fons, C. Levelut, R. Le Parc, M. Hanfland, J. Tominaga, A. Pradel, and M. Ribes, *ibid.* **103**, 115502 (2009); D. A. Baker, M. A. Paesler, G. Lucovsky, S. C. Agarwal, and P. C. Taylor, *ibid.* **96**, 255501 (2006).
[7] S. H. Chang, J. S. Lee, S. C. Chae, S. B. Lee, C. Liu, B. Kahng, D.-W. Kim, and T. W. Noh, Phys. Rev. Lett. **102**, 026801 (2009).
[8] K. E. Petersen and D. Adler, J. Appl. Phys. **47**, 256 (1976).
[9] B. K. Ridely, Proc. Phys. Soc. London **82**, 954 (1963).
[10] J. Ross, *Thermodynamics and Fluctuations Far from Equilibrium* (Springer, New York, 2008), p. 119.
[11] E. Scholl, *Nonequilibrium Phase Transitions in Semiconductors* (Springer, Berlin, 1987).
[12] A. Wacker and E. Scholl, J. Appl. Phys. **78**, 7352 (1995).
[13] A. Alekseev, S. Bose, P. Rodin, and E. Scholl, Phys. Rev. E **57**, 2640 (1998).
[14] P. Rodin, Phys. Rev. B, **69**, 045307 (2004).
[15] A. Redaelli, A. Pirovano, A. Benvenuti, and A. L. Lacaita, J. Appl. Phys. **103**, 11 (2008).
[16] K. E. Petersen and D. Adler, J. Appl. Phys. **50**, 5065 (1979).
[17] M. Nardone, V. G. Karpov, D. C. S. Jackson, and I. V. Karpov, Appl. Phys. Lett. **94**, 103509 (2009).
[18] E. M. Lifshitz and L. P. Pitaevskii, *Physical Kinetics* (Elsevier, Amsterdam, 2008).

[19]M. C. Weinberg and G. F. Nelson, J. Non-Cryst. Solids **74**, 177 (1985); C. Barrett, W. Nix, and A. Tetelmam, *The Principles of Engineering Materials* (Prentice-Hall, Englewood Cliffs, NJ, 1973); X. S. Miao, L. P. Shi, H. K. Lee, J. M. Li, R. Zhao, P. K. Tan, K. G. Lim, H. X. Yang, and T. C. Chong, Jpn. J. Appl. Phys., Part 1 **45**, 3955 (2006).
[20]A. E. Owen and J. M. Robertson, IEEE Trans. Electron Devices **ED-20**, 105 (1973).
[21]I. V. Karpov, M. Mitra, D. Kau, G. Spadini, A. Y. Kryukov, and V. G. Karpov, Appl. Phys. Lett. **92**, 173501 (2008); V. G. Karpov, Y. A. Kryukov, I. V. Karpov, and M. Mitra, Phys. Rev. B **78**, 052201 (2008).
[22]H. Fritzsche, J. Phys. Chem. Solids **68**, 878 (2007).
[23]M. Nardone, V. G. Karpov, and I. V. Karpov, J. Appl. Phys., **107**, 054519 (2010).